

NACA RM L9H17



~~RESTRICTED~~  
~~SECURITY INFORMATION~~

4404

655

C 2

CLASSIFICATION CANCELLED

~~RESTRICTED~~ NACA

To ~~SECURITY INFORMATION~~

By authority of *H. L. Dryden* Date *6-11-53*

# RESEARCH MEMORANDUM

*per NACA Release form #1507.*  
*By HSR, 7-20-53*

LOW-SPEED STATIC LONGITUDINAL STABILITY CHARACTERISTICS

OF A CANARD MODEL HAVING A 60° TRIANGULAR

WING AND HORIZONTAL TAIL

By William R. Bates

Langley Aeronautical Laboratory  
Langley Air Force Base, Va.

CLASSIFICATION CANCELLED

## CLASSIFIED DOCUMENT

This document contains classified information affecting the National Defense of the United States within the meaning of the Espionage Act, USC 50c1 and 52. Its transmission or the revelation of its contents in any manner to an unauthorized person is prohibited by law. Information so classified may be imparted only to persons in the military and naval services of the United States, appropriate civilian officers and employees of the Federal Government who have a legitimate interest therein, and to United States citizens of known loyalty and discretion who of necessity must be informed thereof.

Authority: *J. W. Crowley* Date: *12/14/53*  
*EO 10501*  
*MDA 1/11/54* See *NACA*  
*R 71921*

## NATIONAL ADVISORY COMMITTEE FOR AERONAUTICS

WASHINGTON

November 9, 1949

UNCLASSIFIED

~~RESTRICTED~~  
~~SECURITY INFORMATION~~

~~RESTRICTED~~  
~~SECURITY INFORMATION~~

UNCLASSIFIED

## NATIONAL ADVISORY COMMITTEE FOR AERONAUTICS

## RESEARCH MEMORANDUM

## LOW-SPEED STATIC LONGITUDINAL STABILITY CHARACTERISTICS

OF A CANARD MODEL HAVING A  $60^\circ$  TRIANGULAR

## WING AND HORIZONTAL TAIL

By William R. Bates

## SUMMARY

An investigation of the low-speed, power-off static longitudinal stability and control characteristics of a canard model with a triangular wing and horizontal tail has been conducted in the Langley free-flight tunnel. With the horizontal tail fixed as a nose elevator, the model had essentially no allowable center-of-gravity range when the area of the tail was 8 percent of the wing area, but it had an allowable center-of-gravity range of about 10 percent of the wing mean aerodynamic chord when the area of the tail was 16 percent of the wing area. When the 16-percent horizontal tail was used as a free-floating nose elevator, the allowable center-of-gravity range was about 14 percent of the wing mean aerodynamic chord.

## INTRODUCTION

The NACA has been making a study of canard configurations for high-speed airplanes. Some of the results of this study (reference 1) have indicated that the canard arrangement might have certain advantages over conventional-type airplanes. A suggestion also has been made that a canard arrangement be used with the horizontal tail fixed for supersonic flight and free floating for subsonic flight in order to overcome the difficulties caused by the change in aerodynamic-center location between subsonic and supersonic speeds on triangular-wing airplanes. In order to obtain some general information on the static longitudinal stability of canard airplanes with triangular wings, an investigation of the low-speed, power-off stability and control characteristics of a canard model with a  $60^\circ$  triangular wing and horizontal tail has been made by means of force tests in the Langley free-flight tunnel.

~~RESTRICTED~~  
~~SECURITY INFORMATION~~

UNCLASSIFIED

The data have been analyzed as applied to two types of airplane design: One in which the tail is used simply to overcome the change of stability which results from the change in aerodynamic-center location between subsonic and supersonic speed conditions, and one in which the horizontal tail is used for longitudinal control either with the tail linked directly to the stick as an all-movable control surface or with the tail floating freely and controlled by a servotab.

### SYMBOLS

All forces and moments were referred to the stability axes which are defined in figure 1. The symbols and coefficients used in the present paper are:

S	wing area, square feet
$\bar{c}$	wing mean aerodynamic chord, feet
q	dynamic pressure, pounds per square foot ( $\frac{1}{2}\rho V^2$ )
V	airspeed, feet per second
$\rho$	air density, slugs per cubic foot
$\alpha$	angle of attack of fuselage center line, degrees
$i_t$	angle of incidence of the horizontal tail with respect to the fuselage center line, degrees
$\alpha_t$	angle of attack of the horizontal tail, degrees
$C_L$	lift coefficient (Lift/qS)
$C_D$	drag coefficient (Drag/qS)
$C_m$	pitching-moment coefficient (Pitching moment/qSc)
$\delta_t$	horizontal-tail tab deflection, degrees

### APPARATUS AND TESTS

A three-view drawing of the model used in the present investigation is presented in figure 2. The physical characteristics of the model are presented in table I. Two horizontal tails having areas of 8 percent

and 16 percent of the area of the wing were used in the investigation. The results obtained with the flat-plate airfoil sections used on the model are approximately the same as would have been obtained with a conventional section because the aerodynamic characteristics of delta wings are virtually independent of the airfoil section at low scale. This characteristic has been established by comparison of the aerodynamic characteristics of some flat-plate delta wings from reference 2 with some German data on delta wings (reference 3) having NACA 0012 airfoil sections and with some unpublished data on a 60° delta wing with an NACA 0015-64 airfoil section.

Force tests to determine the aerodynamic characteristics of the model were made on the six-component balance in the Langley free-flight tunnel. These facilities are described in references 4 and 5. All the force tests were made at a dynamic pressure of 3.0 pounds per square foot which corresponds to a Reynolds number of approximately 483,000 based on the wing mean aerodynamic chord.

Tests were made to determine the static longitudinal stability and control characteristics of the model with the horizontal tail off, fixed at various angles of incidence, and floating freely at various tab deflections.

## RESULTS AND DISCUSSION

The longitudinal stability and control characteristics of the model may be analyzed in two ways, depending on the use that is made of the horizontal tail. As previously mentioned, the tail may be used simply to overcome the change of stability which results from the change in aerodynamic-center location between subsonic and supersonic speed conditions. In this case longitudinal control may be obtained by deflecting the ailerons up or down together to serve as an elevator. The horizontal tail also may be used for longitudinal control by linking it to the stick as an all-movable surface or by varying the angle of attack of a free-floating tail with a servotab. The method of analysis of the data is quite different, depending on which of these two uses is made of the horizontal tail. The discussion of the longitudinal stability and control characteristics of the model has been divided into two parts, therefore, to separate the analysis of the data as applied to airplanes using the horizontal tail for the two different purposes.

### Horizontal Tail Used to Overcome Change in Stability

When the horizontal tail is used simply as a device to overcome the change in stability between subsonic and supersonic speeds, it is

allowed to float freely at  $0^\circ$  tab deflection at subsonic speeds and is fixed at supersonic speeds. By using the horizontal tail in this way, it should be possible to have the aerodynamic center of an airplane in approximately the same position at both subsonic and supersonic speeds. The change in aerodynamic-center location between the tail-free and tail-fixed conditions at subsonic speeds for the 8-percent and 16-percent horizontal tails can be determined from the data presented in figures 3 and 4. Since the slope of the lift curve  $C_{L_\alpha}$  of a  $60^\circ$  delta wing is about the same at subsonic and supersonic speeds, these data should give an approximate determination of the size of the tail required to keep the aerodynamic center in the same position at both subsonic and supersonic speeds. It is not known, however, just what would happen to the stability characteristics in going from subsonic to supersonic speeds because of the interference of compressibility effects.

The data presented in figures 3 and 4 indicate that the aerodynamic center of the model varied slightly with lift coefficient. For the present analysis, therefore, the aerodynamic center of the model was determined from the slope of the pitching-moment curve  $\frac{dC_m}{dC_L}$  at zero

lift. The aerodynamic center of the model having the 8-percent horizontal tail was located at  $0.37\bar{c}$  with the tail free and at  $0.23\bar{c}$  with the tail fixed at  $0^\circ$  incidence — a change in aerodynamic-center location of  $0.14\bar{c}$  between the tail-fixed and tail-free conditions. The aerodynamic center of the model having the 16-percent horizontal tail was located at  $0.45\bar{c}$  with the tail free and at  $0.13\bar{c}$  with the tail fixed at  $0^\circ$  incidence — a change in aerodynamic-center location of  $0.32\bar{c}$  between the tail-fixed and tail-free conditions. NACA tests on a model similar to that used in the present investigation show that the change in aerodynamic-center location between subsonic and supersonic speeds for the model without the horizontal tail is about  $0.08\bar{c}$  or  $0.10\bar{c}$ . For this change in aerodynamic-center location, a horizontal tail having an area of about 6 percent of the wing area would probably be required to keep the aerodynamic center of this design at about the same position for both subsonic and supersonic speeds.

#### Horizontal Tail Used for Longitudinal Control

For the case in which the horizontal tail is used to obtain longitudinal control by varying the angle of incidence with the tail fixed or the tab deflection with the tail floating freely, the longitudinal stability and control characteristics of the model with various horizontal-tail arrangements are compared on the basis of the center-of-gravity range for which the model was longitudinally stable and for which the model could be trimmed to its maximum lift coefficient without the horizontal tail. This range of center-of-gravity locations is

referred to herein as the allowable center-of-gravity range. One limit was taken as the farthest rearward center-of-gravity location at which the model was at least neutrally stable over the entire lift-coefficient range with neutral controls. The other limit was taken as the most forward center-of-gravity location at which the model would trim to the maximum lift coefficient of the model without the horizontal tail ( $C_L = 1.0$ ). The allowable center-of-gravity range of the  $60^\circ$  delta-wing model need be only about half that of a conventional model when expressed as a fraction of the mean aerodynamic chord because the length of the mean aerodynamic chord of the delta wing is about twice that of a wing of normal aspect ratio having the same area.

Fixed tail.— Analysis of figure 3 shows that, with the 8-percent horizontal tail fixed, the model had essentially no allowable center-of-gravity range because the tail is virtually ineffective for trimming to high lift coefficients. The most rearward center-of-gravity position for which the model is neutrally stable and the most forward center-of-gravity position for which the model can be trimmed to a lift coefficient of 1.0 are approximately the same. The data presented in figure 5(a) show that the 8-percent horizontal tail was ineffective for trimming to high lift coefficients because the tail was more effective for stability than for trim; that is, the variation of horizontal-tail pitching moment is greater for a change in angle of attack than for a change in tail incidence. This results primarily from the fact that the gap in the horizontal tail increases as the tail incidence increases so that the tail lift-curve slope is lower when the incidence is varied than when the angle of attack is varied.

With the 16-percent tail fixed, the model had an allowable center-of-gravity range of about  $0.10\bar{C}$ . Analysis of the pitching-moment data presented in figure 6 shows that the model was neutrally stable with the center of gravity at approximately  $0.10\bar{C}$  and could not be trimmed to the maximum lift of the model without the horizontal tail ( $C_L = 1.0$ ) when the center of gravity was forward of the leading edge of the mean aerodynamic chord. There are probably several reasons that the 16-percent tail gave a larger allowable center-of-gravity range than the 8-percent tail. One reason is simply its larger size which causes it to produce larger pitching moments and also causes the losses due to opening the gap to be smaller in proportion to the tail size. The data of figure 5(b) also indicate that the interference effects on the 16-percent tail at high angles of attack, unlike those on the 8-percent tail, cause it to produce larger pitching moments with tail incidences of  $7^\circ$ ,  $10^\circ$ , and  $15^\circ$  than with  $0^\circ$ .

Free-floating tail.— The longitudinal stability characteristics of the model with the 16-percent horizontal tail as a free-floating nose elevator are presented in figure 7. The effect on the pitching-moment

coefficient of varying the center of gravity is presented in figure 8. Analysis of this figure shows that the allowable center-of-gravity range of the model with the tail floating freely was approximately 0.136. The model was neutrally stable with the center of gravity approximately 0.276 and could be trimmed to the maximum lift coefficient of the model without the horizontal tail ( $C_L = 1.0$ ) when the center of gravity was behind approximately 0.146. Two factors that might account for the free-floating horizontal tail being more effective than the fixed tail for trimming to high lift coefficients are that the moment arm of the horizontal tail is longer when the tail is free than when the tail is fixed because of the more rearward location of the neutral point for the tail-free configuration and that, for trim conditions, the gap in the horizontal tail is smaller when the tail is free than when the tail is fixed because of the smaller incidence required for trim in the tail-free condition.

#### CONCLUSIONS

The following conclusions were drawn from an investigation in the Langley free-flight tunnel on a canard model to determine static longitudinal stability and control characteristics:

1. With the horizontal tail fixed as an all-movable control surface, the model had essentially no allowable center-of-gravity range when the area of the tail was 8 percent of the wing area, but it had an allowable center-of-gravity range of about 10 percent of the wing mean aerodynamic chord when the area of the tail was 16 percent of the wing area.

2. When the 16-percent horizontal tail was used as a free-floating nose elevator, the allowable center-of-gravity range was about 14 percent of the wing mean aerodynamic chord.

Langley Aeronautical Laboratory  
National Advisory Committee for Aeronautics  
Langley Air Force Base, Va.

## REFERENCES

1. Mathews, Charles W.: Study of the Canard Configuration with Particular Reference to Transonic Flight Characteristics at High Lift. NACA RM L8G14, 1948.
2. Tosti, Louis P.: Low-Speed Static Stability and Damping-in-Roll Characteristics of Some Swept and Unswept Low-Aspect-Ratio Wings. NACA TN 1468, 1947.
3. Lange and Wacke: Test Report on Three- and Six-Component Measurements on a Series of Tapered Wings of Small Aspect Ratio (Partial Report: Triangular Wing). NACA TM 1176, 1948.
4. Shortal, Joseph A., and Osterhout, Clayton J.: Preliminary Stability and Control Tests in the NACA Free-Flight Wind Tunnel and Correlation with Full-Scale Flight Tests. NACA TN 810, 1941.
5. Shortal, Joseph A., and Draper, John W.: Free-Flight-Tunnel Investigation of the Effect of the Fuselage Length and the Aspect Ratio and Size of the Vertical Tail on Lateral Stability and Control. NACA ARR 3D17, 1943.

14c  
13c



TABLE I.— DIMENSIONAL CHARACTERISTICS OF THE CANARD MODEL WITH  
A TRIANGULAR WING TESTED IN THE LANGLEY FREE-FLIGHT TUNNEL

## Wing:

Area, sq ft . . . . .	2.95
Span, ft . . . . .	2.61
Aspect ratio . . . . .	2.31
Mean aerodynamic chord, ft . . . . .	1.505
Sweepback of leading edge . . . . .	60
Dihedral (relative to mean thickness line), deg . . . . .	0
Taper ratio (tip chord/root chord) . . . . .	0
Airfoil section . . . . .	Flat plate

## Elevon:

Type . . . . .	Plain
Area (one), sq ft . . . . .	0.268
Span (at trailing edge of wing, one), ft . . . . .	1.14
Chord (from hinge line to trailing edge), ft . . . . .	0.254

## Horizontal tail (16 percent):

Area, sq ft . . . . .	0.472
Span, ft . . . . .	1.045
Aspect ratio . . . . .	2.31
Sweepback of leading edge, deg . . . . .	60
Tab area, sq ft . . . . .	0.1062
Tab chord, ft . . . . .	0.1042
Airfoil section . . . . .	Flat plate
Distance from center of gravity to tail hinge line, ft . . . . .	1.027

## Vertical tail:

Area, sq ft . . . . .	0.527
Height, ft . . . . .	0.78
Aspect ratio . . . . .	1.155
Sweepback of leading edge, deg . . . . .	60
Taper ratio (tip chord/root chord) . . . . .	0
Rudder area, sq ft . . . . .	0.1055
Rudder chord, ft . . . . .	0.1425
Airfoil section . . . . .	Flat plate
Tail length (distance from c.g. to center of area), ft . . . . .	0.830



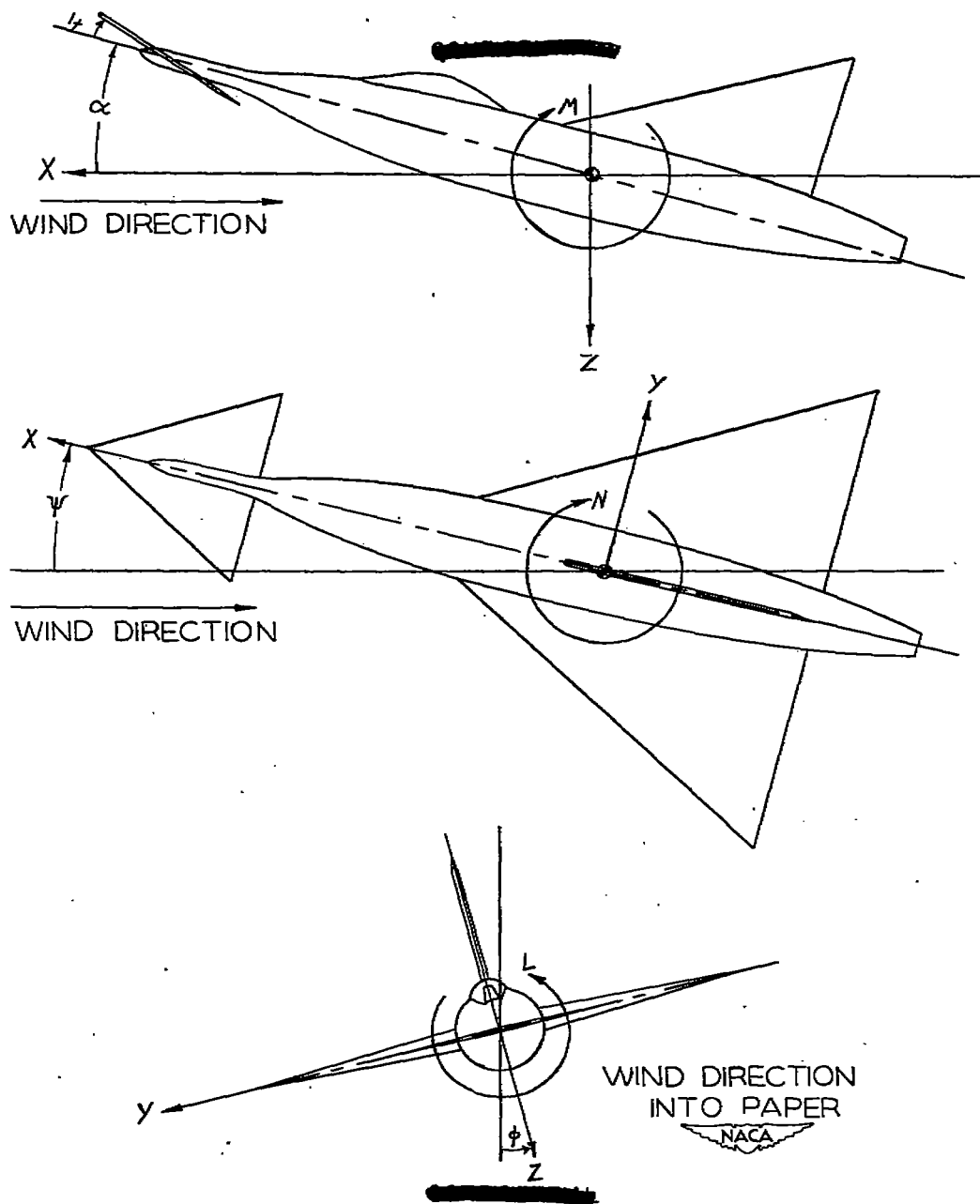


Figure 1.— The stability system of axes. Arrows indicate positive directions of moments, forces, and control-surface deflections. This system of axes is defined as an orthogonal system having their origin at the center of gravity and in which the Z-axis is in the plane of symmetry and perpendicular to the relative wind, the X-axis is in the plane of symmetry and perpendicular to the Z-axis, and the Y-axis is perpendicular to the plane of symmetry.

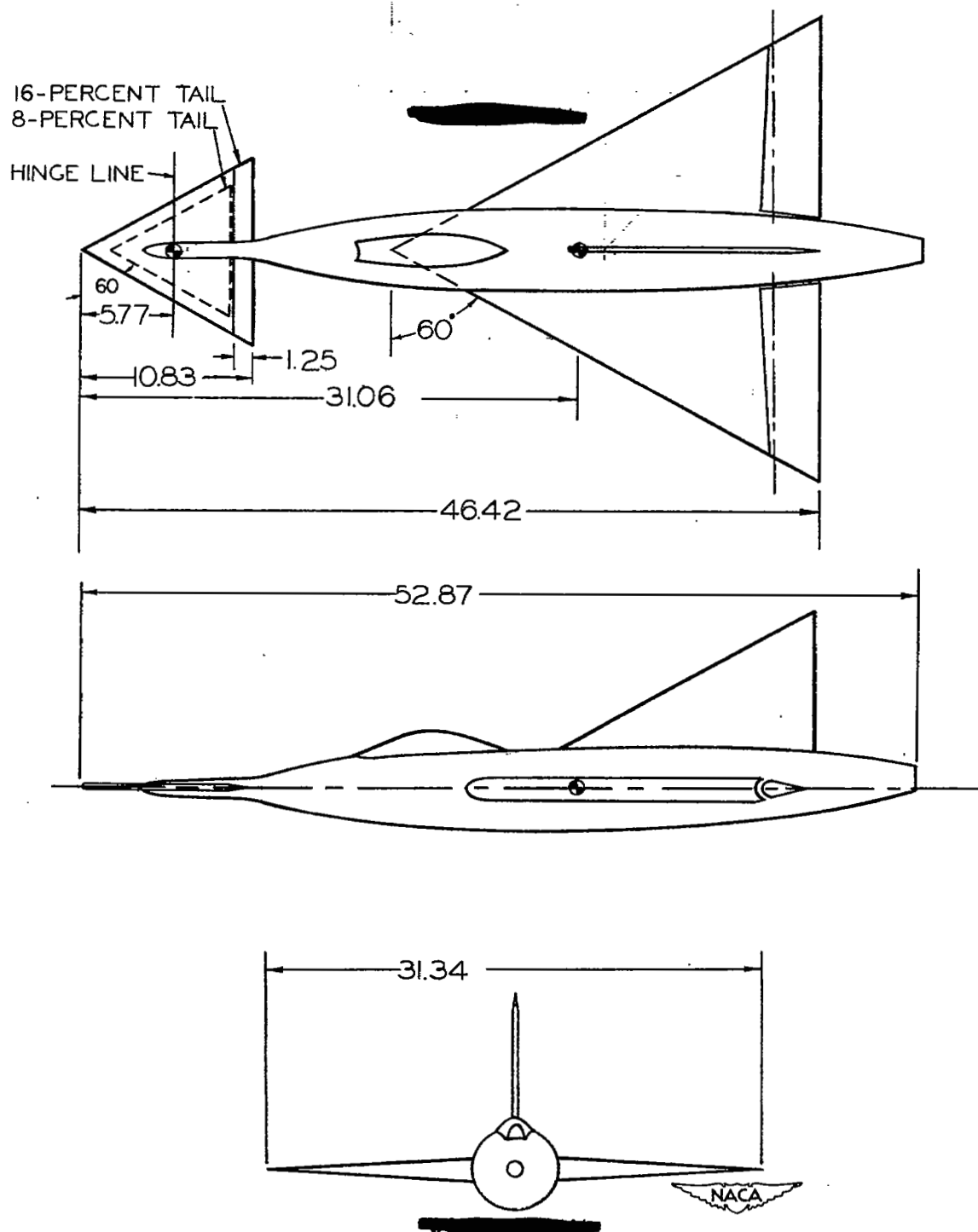


Figure 2.— Three-view drawing of the model showing the various horizontal- and vertical-tail configurations.

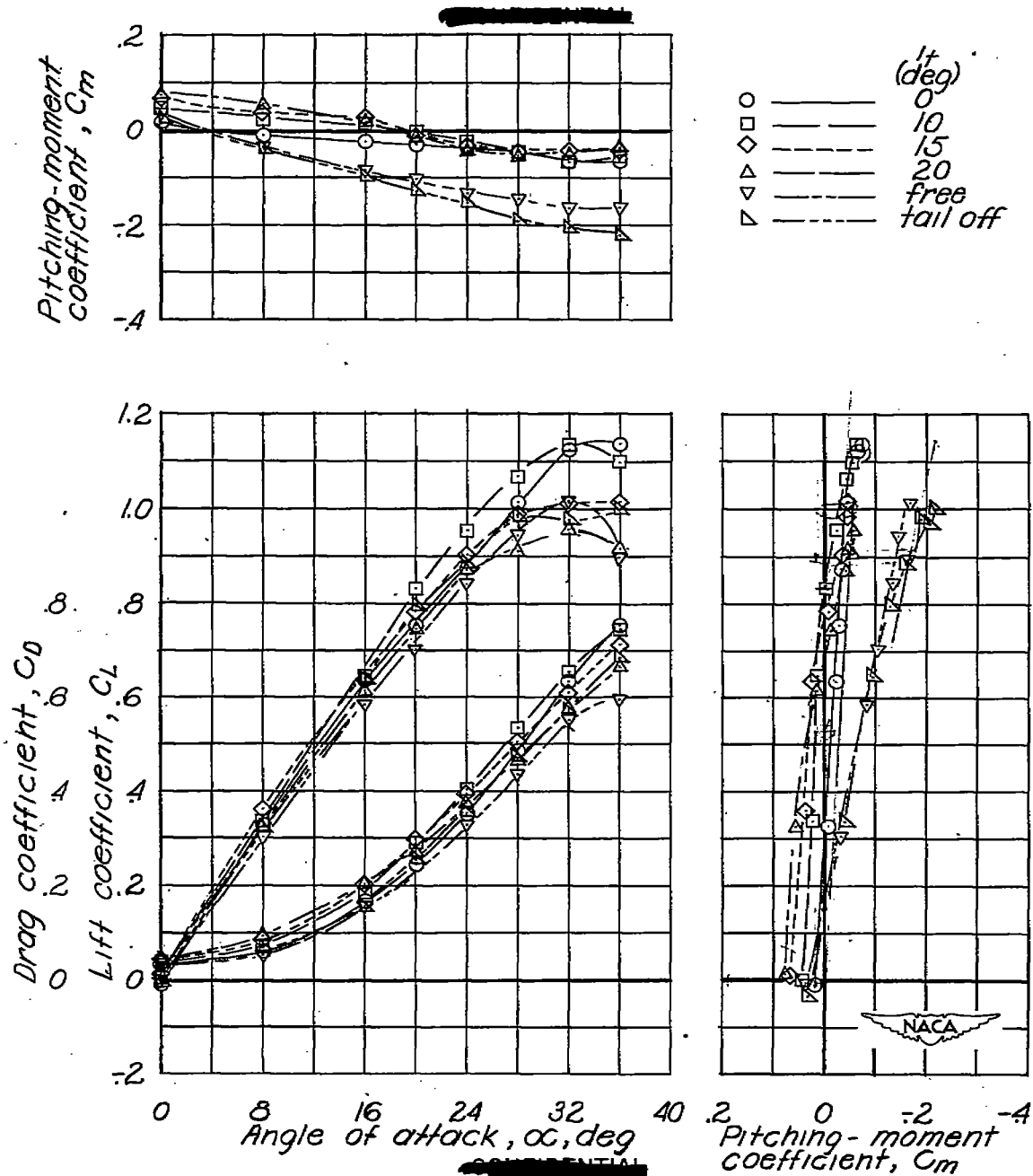


Figure 3.— Longitudinal stability characteristics of the model with the 8-percent horizontal tail fixed at various angles of incidence. (Center vertical tail.)

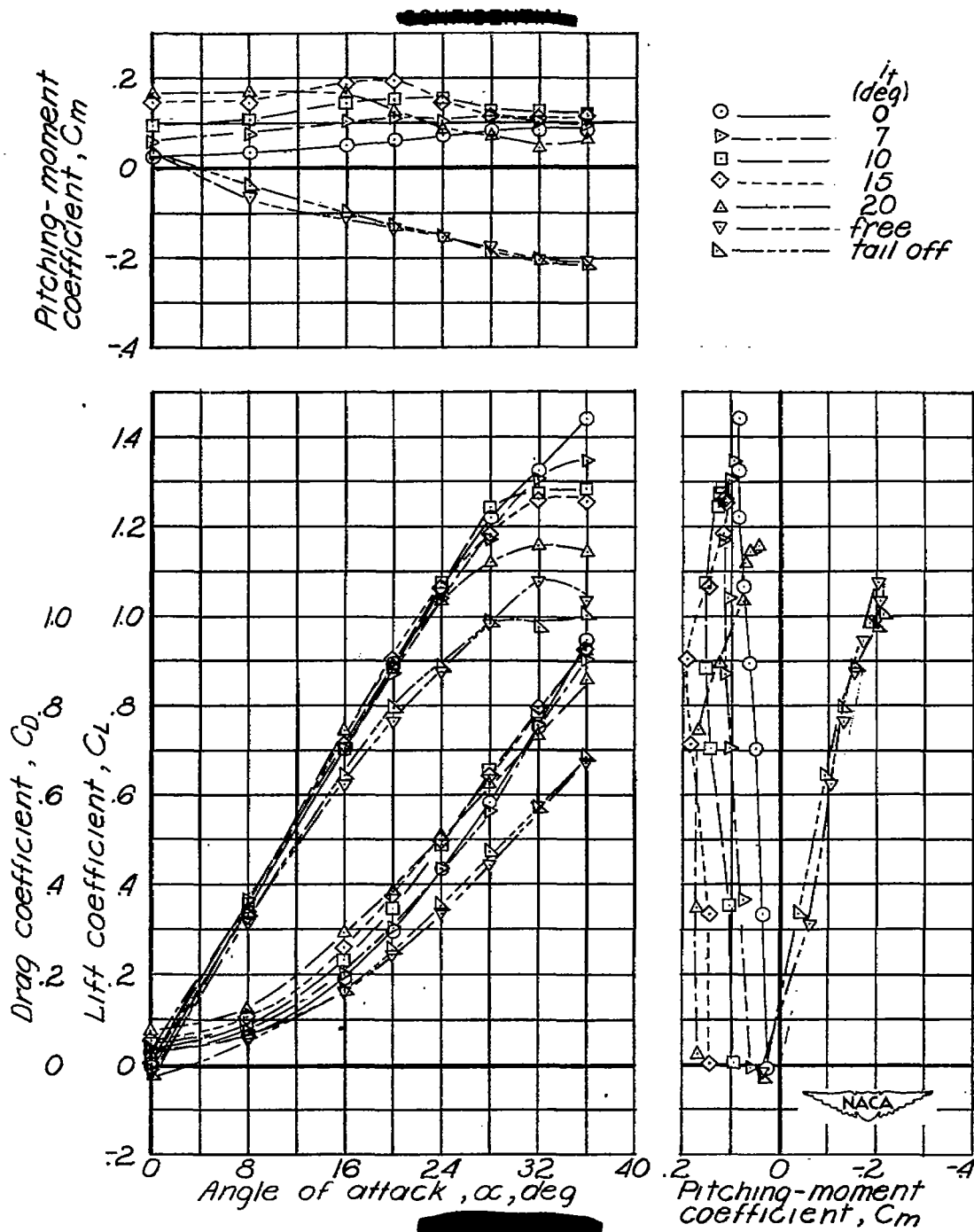


Figure 4.— Longitudinal stability characteristics of the model with the 16-percent horizontal tail fixed at various angles of incidence. (Center vertical tail.)

L.S. @ 157.5

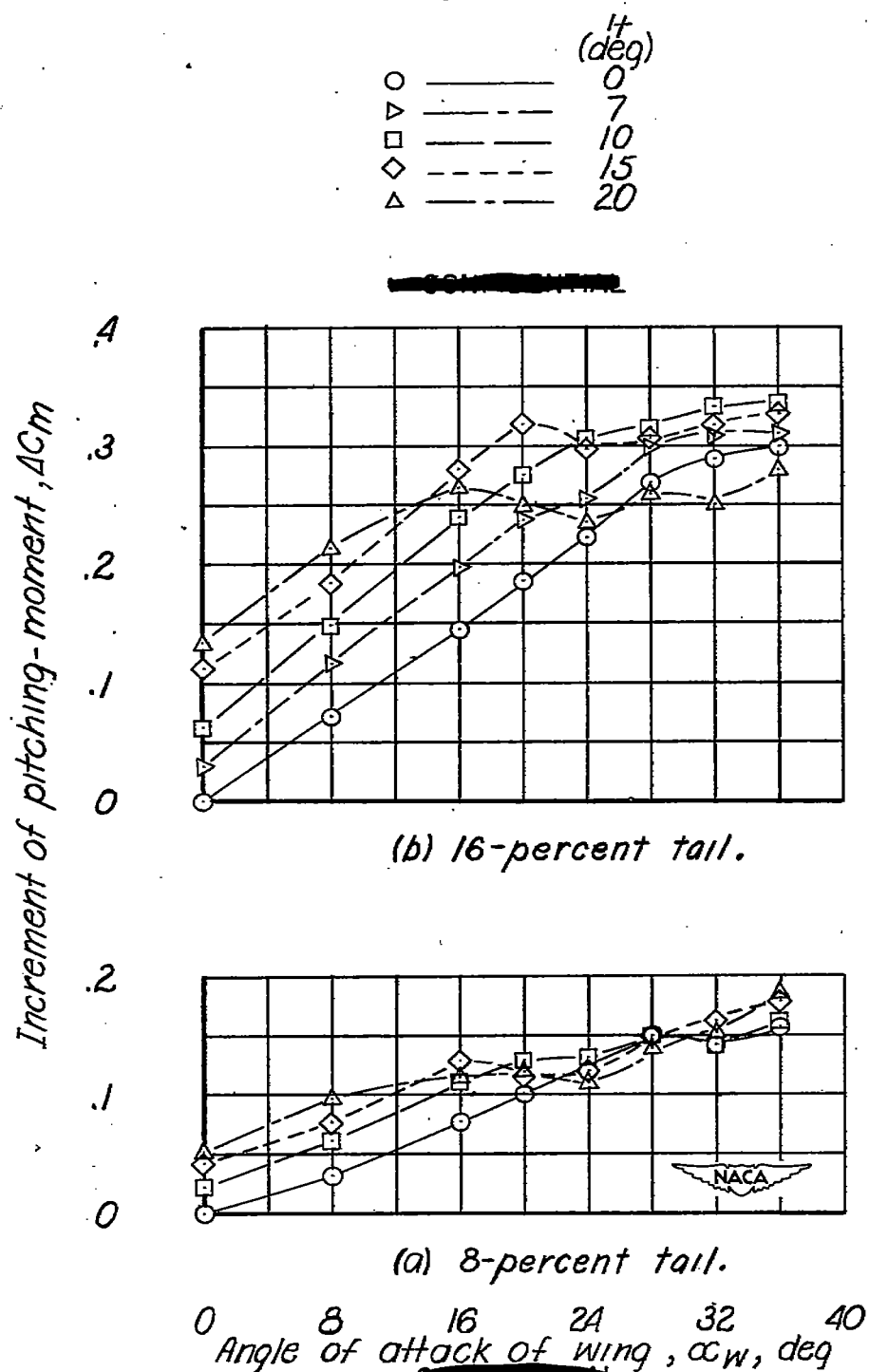


Figure 5.— Increments of pitching moment caused by the horizontal tail at various angles of tail incidence.

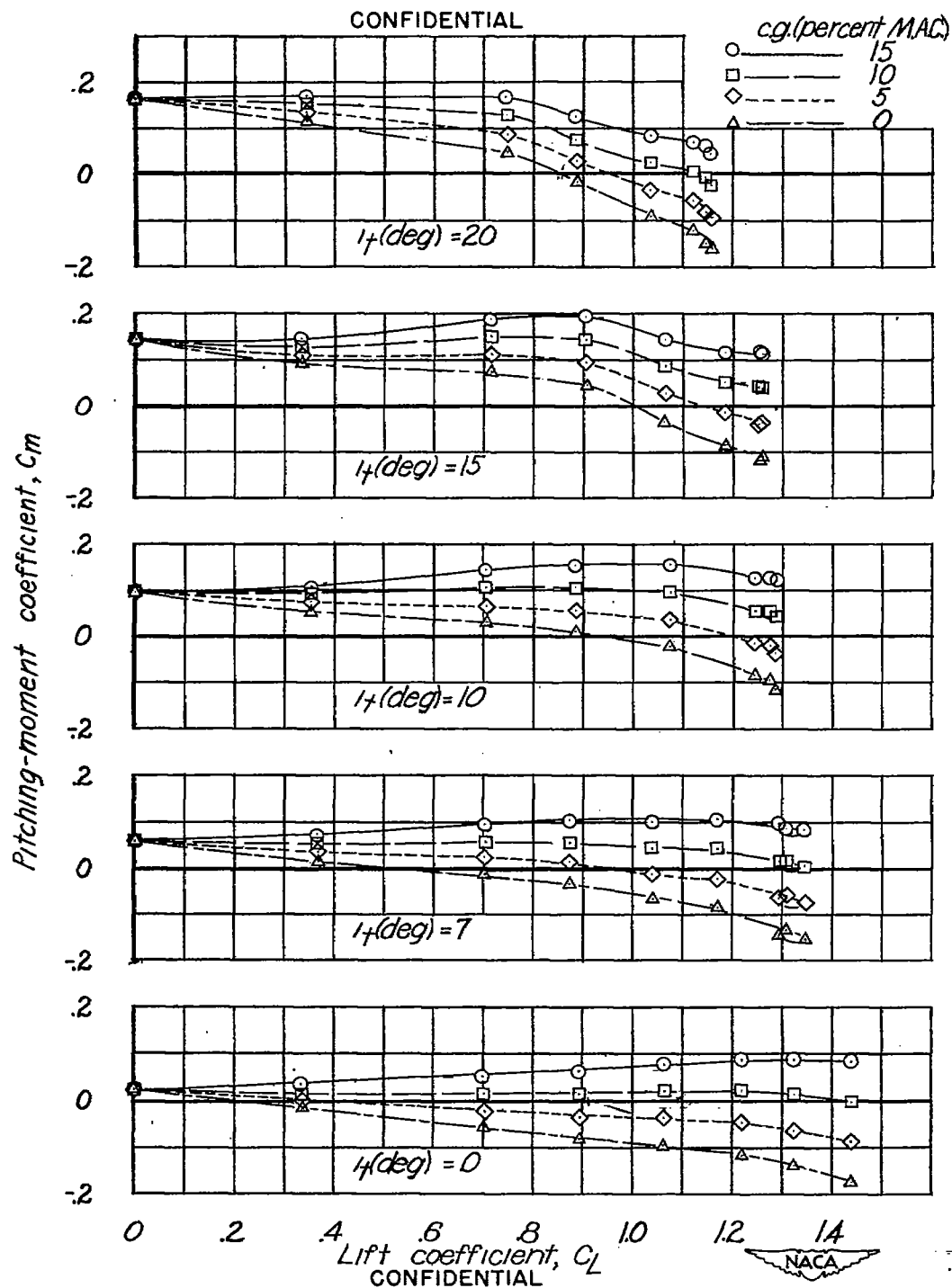


Figure 6.— Pitching-moment coefficients at various center-of-gravity locations for the model with the 16-percent horizontal tail fixed at various angles of incidence. (Center vertical tail.)

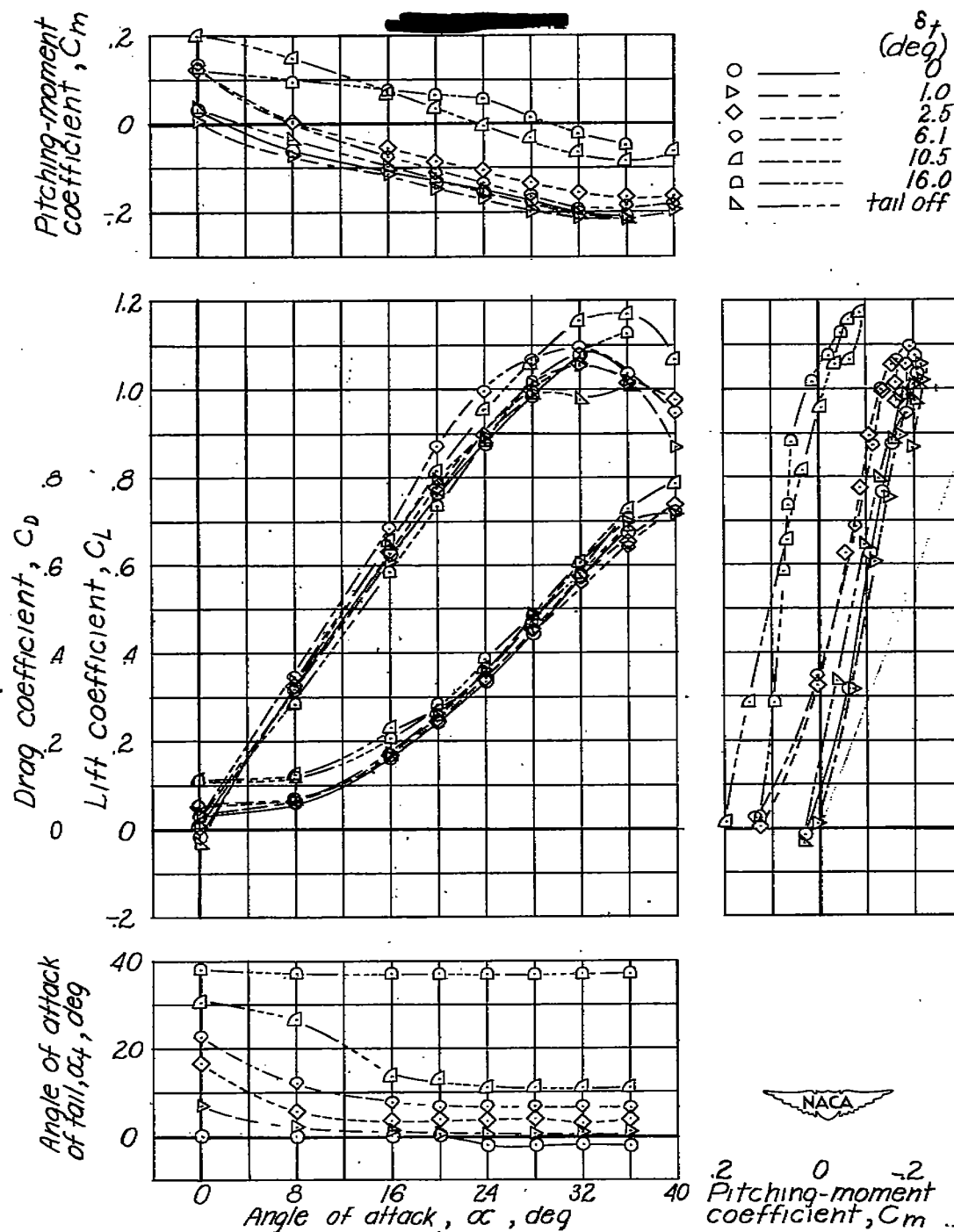


Figure 7.— Longitudinal stability characteristics of the model with the 16-percent horizontal tail floating freely at various tab deflections. (Center vertical tail.)



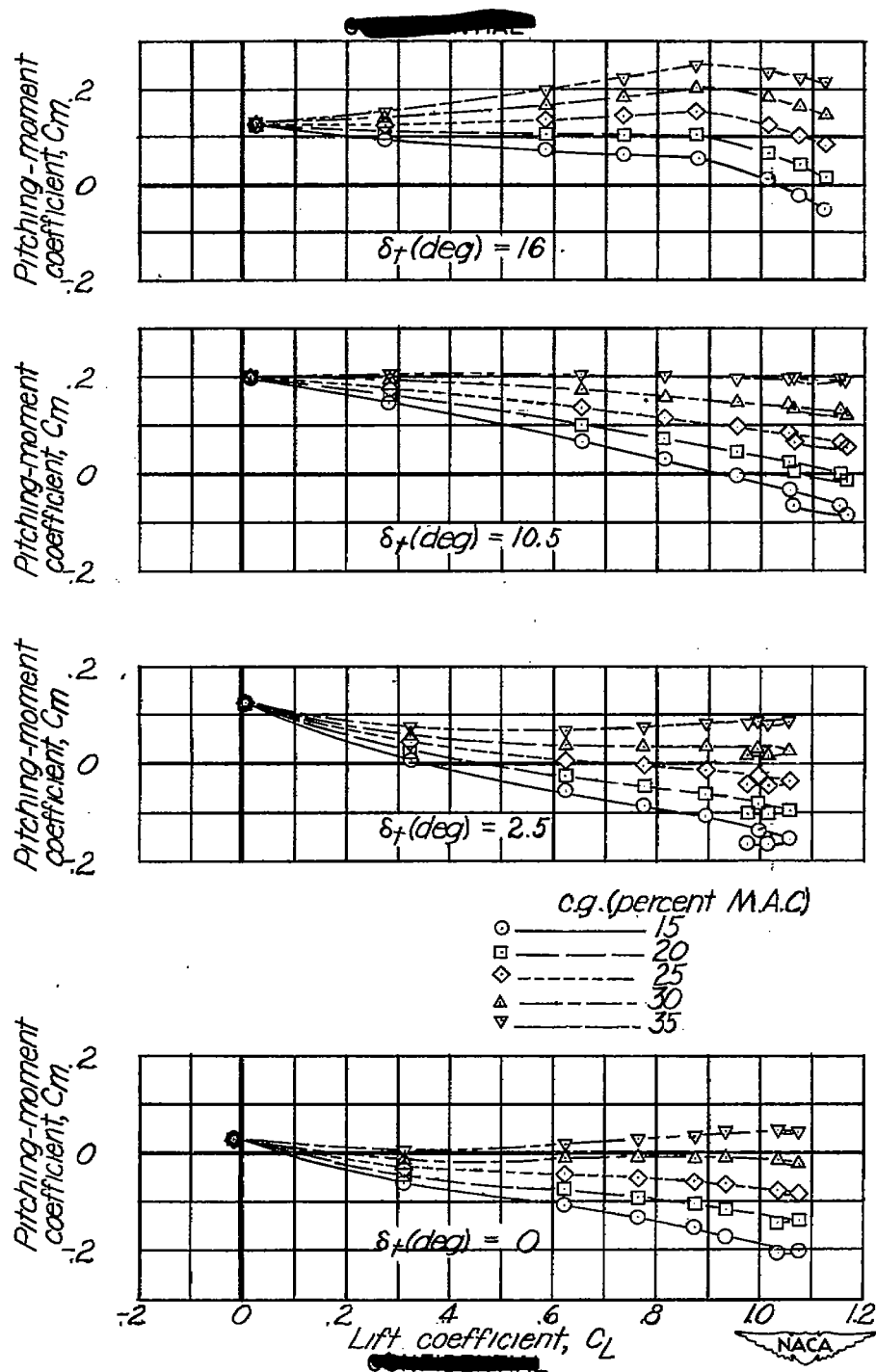


Figure 8.— Pitching-moment coefficients at various center-of-gravity locations for the model with the 16-percent horizontal tail floating freely at various tab deflections. (Center vertical tail.)